1521-0111/12/8101-63–72$25.00
MOLECULAR PHARMACOLOGY
Vol. 81, No. 1
75192/3738215

Mol Pharmacol 81:63–72, 2012

Modeling Human Cytochrome P450 2D6 Metabolism and Drug-Drug Interaction by a Novel Panel of Knockout and Humanized Mouse Lines[S]

Nico Scheer, Yury Kapelyukh, Jillian McEwan, Vincent Beuger, Lesley A. Stanley, Anja Rode, and C. Roland Wolf

TaconicArtemis, Köln, Germany (N.S., V.B., A.R.); CXR Biosciences Limited, Dundee, United Kingdom (Y.K., J.M., C.R.W.); Consultant in Investigative Toxicology, St. Andrews, Fife, United Kingdom (L.A.S.); and Cancer Research U.K. Molecular Pharmacology Unit, Biomedical Research Institute, Ninewells Hospital and Medical School, University of Dundee, Dundee, United Kingdom (C.R.W.)

Received August 12, 2011; accepted October 11, 2011

ABSTRACT

The highly polymorphic human cytochrome P450 2D6 enzyme is involved in the metabolism of up to 25% of all marketed drugs and accounts for significant individual differences in response to CYP2D6 substrates. Because of the differences in the multiplicity and substrate specificity of CYP2D family members among species, it is difficult to predict pathways of human CYP2D6-dependent drug metabolism on the basis of animal studies. To create animal models that reflect the human situation more closely and that allow an in vivo assessment of the consequences of differential CYP2D6 drug metabolism, we have developed a novel straightforward approach to delete the entire murine *Cyp2d* gene cluster and replace it with allelic variants of human *CYP2D6*. By using this approach, we have generated mouse lines expressing the two frequent human protein isoforms CYP2D6.1 and CYP2D6.2 and an as yet undescribed variant of this enzyme, as well as a *Cyp2d* cluster knockout mouse. We demonstrate that the various transgenic mouse lines cover a wide spectrum of different human CYP2D6 metabolizer phenotypes. The novel humanization strategy described here provides a robust approach for the expression of different *CYP2D6* allelic variants in transgenic mice and thus can help to evaluate potential CYP2D6-dependent interindividual differences in drug response in the context of personalized medicine.

Introduction

Cytochromes P450 are heme-containing enzymes responsible for the oxidative metabolism of a wide variety of small molecule substrates. Human CYP2D6 is one of the major members of the cytochrome P450 superfamily. It plays a central role in the metabolism of up to 25% of drugs in common clinical use, as well as a variety of endogenous compounds (Yu et al., 2004; Zanger et al., 2004). CYP2D6 is highly polymorphic, and more than 100 allelic variants have been detected (http://www.cypalleles.ki.se/cyp2d6.htm). As a consequence, CYP2D6 activities vary significantly among individuals. Some of the CYP2D6 alleles are nonfunctional and do not produce an active CYP2D6 protein (Gough et al., 1990), resulting in the so-called poor metabolizer phenotype in 5 to 10% of the white population (Gonzalez et al., 1988; Brockmöller and Tzvetkov, 2008). *CYP2D6*1* and **2* are the most frequent alleles in whites, and they are associated with the extensive metabolizer phenotype (Sachse et al., 1997; Sakuyama et al., 2008). In addition, several alleles account for either intermediate or ultrarapid metabolizer phenotypes (Sachse et al., 1997). Significant differences in the frequencies of the allelic variants do exist in different ethnic groups (Bradford, 2002). Such differences in the genotype can result in significantly altered metabolism of certain classes of drugs such as antidepressants and antihypertensive drugs (de Leon et al., 2006; Eichelbaum et al., 2006; Thuerauf and Lunkenheimer, 2006). The poor metabolizer phenotype has also been linked to reduced efficacy of the anticancer drug tamoxifen (Brauch et al., 2009; Hoskins et al., 2009).

To avoid later stage drug attrition and to rank compounds according to their developability, the pharmacokinetics and bioavailability of new chemical entities are being evaluated

This work was supported in part by ITI Life Sciences, Scotland.
Article, publication date, and citation information can be found at http://molpharm.aspetjournals.org.
http://dx.doi.org/10.1124/mol.111.075192.
[S] The online version of this article (available at http://molpharm.aspetjournals.org) contains supplemental material.

ABBREVIATIONS: WT, wild-type; kb, kilobase(s); ES, embryonic stem; KO, knockout; HLM, human liver microsomes; AUC, area under the concentration-time curve; MR, metabolic ratio.

early in drug discovery. A major challenge in the extrapolation of animal data to humans lies in species differences in the structure and function of the major xenobiotic receptors, transporters, and drug-metabolizing enzymes (Lin, 2008). For example, the only functional *CYP2D* gene in humans is *CYP2D6*, compared with nine functional genes in the mouse (Nelson et al., 2004). Furthermore, recent studies revealed marked differences in the substrate specificities between murine Cyp2d22 or Cyp2d9 on the one hand and human CYP2D6 on the other (Smith et al., 1998; McLaughlin et al., 2008).

A robust approach to generate mouse models humanized for different allelic variants of *CYP2D6* would therefore be of great value in estimating the in vivo role of this enzyme in drug metabolism and drug-drug interactions and to uncover potential interindividual differences in drug response. A mouse line with a random integration of human *CYP2D6* into the mouse genome expressing a functionally active CYP2D6 protein in the liver, kidney, and small intestine has been described previously (Corchero et al., 2001; Miksys et al., 2005). By comparing the elimination rate of the CYP2D6 probe substrate debrisoquine and the formation of the 4-hydroxydebrisoquine metabolite, it was proposed that WT and CYP2D6-humanized mice could be used as models for human poor and extensive metabolizers, respectively (Corchero et al., 2001; Yu et al., 2004; Miksys et al., 2005; Cheung and Gonzalez, 2008). A limitation of this approach, however, is the presence of the murine *Cyp2d* genes in this model. Some of the mouse Cyp2d enzymes have the ability to metabolize CYP2D6 substrates at considerable rates (Bogaards et al., 2000; McLaughlin et al., 2008), so that WT mice do not generically represent the human "poor metabolizer" phenotype. Furthermore, because of the variability among random transgenic lines as a result of the integration at different sites of the genome, it is difficult to standardize this approach as required for a comparison between lines expressing different allelic variants.

For that reason we developed a robust strategy that allowed us to replace the nine functional genes of the mouse *Cyp2d* cluster with different allelic variants of human *CYP2D6* by targeted transgenesis. Three CYP2D6-humanized mouse lines expressing the two frequent protein isoforms CYP2D6.1 and CYP2D6.2 and a novel, as yet unidentified, variant of this enzyme were generated by this approach. All the mouse lines expressed high levels of CYP2D6 in the liver and intestine. In addition, we generated a murine *Cyp2d* cluster knockout model and provide metabolic evidence that this knockout line reflects the human poor metabolizer phenotype. Finally, we show that the putatively new *CYP2D6* allelic variant expresses a protein with low catalytic activity and that, as expected, the CYP2D6.1 and CYP2D6.2 isoforms extensively metabolize different CYP2D6 probe substrates.

Materials and Methods

Animal Husbandry. Mice were kept as described previously (Scheer et al., 2008).

DNA Constructs and Cloning. For targeting the *Cyp2d26* gene locus, a basic vector containing a hygromycin and ZsGreen expression cassette and a splice acceptor polyA motif, a *loxP*, *lox5171*, and *frt* site was constructed in pBluescript. A 5.8-kb genomic sequence immediately upstream from the translational start site of the mouse *Cyp2d26* gene and a 3.7-kb fragment comprising exons 5 to 9 of *Cyp2d26*, both used as targeting arms for homologous recombination, were obtained by red/ET recombineering (Zhang et al., 1998) and subcloned into the basic targeting vector as depicted in Fig. 1C.

For targeting the *Cyp2d22* gene locus to generate humanized CYP2D6.N (hCYP2D6.N) mice, a vector containing a CYP2D6, a neomycin and ZsGreen expression cassette, and a *loxP* and *f3* site was constructed in pACYC. The human CYP2D6 expression cassette contained a contiguous genomic fragment of a 9.0-kb promoter sequence, all exons and introns, and a 700-bp 3′ untranslated region followed by a polyA motif. A 3.9-kb genomic sequence comprising exons 6 to 10 of the mouse *Cyp2d22* gene and a 5.7-kb fragment comprising exons 2 and 3 of *Cyp2d22*, both used as targeting arms for homologous recombination, as well as the genomic human *CYP2D6* fragment were obtained by red/ET recombineering and subcloned into the basic targeting vector as depicted in Fig. 1C. The identification number of the bacterial artificial chromosome used to extract the genomic *CYP2D6* fragment is RP11-142E17 (clone identification number RPCIB753E17142Q; ImaGenes GmbH, Germany). Sequencing of the genomic fragment revealed that it contains naturally occurring polymorphisms in exons 2, 6, and 9. These polymorphisms lead to the nucleotide transitions 1023C>T and 2850C>T, which are associated with the amino acid exchanges T107I and R296C in exons 2 and 6, and a gene conversion to CYP2D7 in exon 9, resulting in the amino acid exchanges P469A, T470A, H478S, G479A, F481V, A482S, and S486T (http://www.cypalleles.ki.se/cyp2d6.htm) (Supplemental Fig. 1). The nucleotide transitions in the hCYP2D6.N targeting vector were corrected by standard molecular cloning techniques to generate hCYP2D6.1 and hCYP2D6.2 targeting vectors.

Generation and Molecular Characterization of Targeted Embryonic Stem Cells. Culture and targeted mutagenesis of embryonic stem (ES) cells were performed as described previously (Hogan et al., 1994). Details on the generation and molecular characterization of ES cell clones targeted at *Cyp2d26* and *Cyp2d22* gene loci are described in the Supplemental Materials and Methods.

Generation and Molecular Characterization of CYP2D6-Humanized and Cyp2d Knockout Mice. *Cyp2d* double-targeted ES clones with targeting on the same allele were expanded, injected into BALB/c blastocysts, and transferred into foster mothers as described previously (Hogan et al., 1994). Litters from these foster mothers were inspected visually, and chimerism was determined by hair color. Highly chimeric animals were used for breeding with a Cre-deleter strain carrying a transgene that expresses Cre in the germ line to delete the mouse *Cyp2d* cluster and to generate CYP2D6-humanized mice (Fig. 1E). Cyp2d knockout (KO) mice were generated by crossing hCYP2D6.N mice to an efficient flipase (Flpe) deleter strain carrying a transgene that expresses Flpe in the germ line, which leads to a deletion of the CYP2D6 expression cassette in the offspring (Fig. 1F). The Cre- and Flpe deleter strains described were both generated in-house on a C57BL/6 genetic background. A detailed description of the molecular characterization of the CYP2D6-humanized and Cyp2d KO mice is given in the Supplemental Materials and Methods.

Animal Experimentation. All animal procedures were performed under a United Kingdom Home Office license, and all animal studies were approved by the Ethical Review Committee, University of Dundee. Homozygous mice for each transgenic line were used for experimental studies, except as noted otherwise. C57BL/6 animals of the same age purchased from Harlan UK Limited (Bicester, Oxon, UK) were used as WT controls. Mice were housed on sawdust in solid-bottom, polypropylene cages and provided with RM1 pelleted diet (Special Diet Services Ltd., Stepfield, Witham, Essex, UK) and drinking water ad libitum before and throughout the study. The temperature was maintained within the range of 19 to 23°C and relative humidity within the range of 40 to 70%. A 12-h light/dark cycle was maintained. The mice were allowed to acclimatize for a minimum of 5 days before use in experiments.

Terminal Procedures. Up to 24 h after treatment, mice were killed by exposure to a rising concentration of CO_2, and blood was

collected by cardiac puncture into lithium/heparin-coated tubes for plasma preparation. Details on the procedures of tissue preparation, immunoblot analysis of Cyp2d and CYP2D6 apoprotein expression, quantitative reverse transcriptase-polymerase chain reaction and in vitro determination of CYP2D-dependent activities are given in the Supplemental Materials and Methods.

Pharmacokinetic Analysis. Food was withdrawn overnight before the initiation of pharmacokinetic analysis. Debrisoquine sulfate (1.95 mg/kg base) and bufuralol hydrochloride (10 mg/kg base) were administered by oral gavage. The vehicle used was sterile water, and the volume of dosing solution was 10 ml/kg b.wt. Details on the pharmacokinetics analysis for debrisoquine and bufuralol and the simulation of bufuralol pharmacokinetics in humans are described in the Supplemental Materials and Methods.

Results

Generation of CYP2D6-Humanized and Cyp2d Cluster Knockout Mice. To replace the nine functional genes of the murine *Cyp2d* cluster with different allelic variants of human *CYP2D6*, we developed a novel strategy of inserting a human expression cassette and subsequently deleting a large fragment of genomic mouse DNA. This approach is illustrated in Fig. 1. In short, the mouse *Cyp2d* cluster was flanked with Cre recombinase recognition (*loxP*) sites by conducting two consecutive rounds of targeting in mouse ES cells, resulting in double-targeted ES cells (Fig. 1, A–D). One of the targeting vectors used to introduce the *loxP* sites also contained the CYP2D6 expression cassette, including 9 kb of promoter, which contains all the intervening region between CYP2D6 and the pseudogene CYP2D7, all exons and introns, and a 700-bp 3′ untranslated region of human *CYP2D6* followed by a polyA motif. A splice acceptor polyA motif was included in the other targeting vector to terminate any potential transcription from the *Cyp2d26* promoter. Transgenic mice from double-targeted ES cells were generated subsequently and by further crosses with a mouse line expressing the Cre recombinase in the germ line, the mouse *Cyp2d* cluster was deleted in vivo by Cre-mediated recombination at the *loxP* sites (Fig. 1E). The additional inclusion of Flp recombinase recognition (*frt*) sites in the targeting vector allowed the subsequent deletion of the human CYP2D6 expression cassette by crossing the humanized mice with a mouse line expressing the Flp recombinase in the germ line, resulting in a complete knockout of the mouse *Cyp2d* Cluster (Fig. 1F). Homozygous humanized and knockout mice were obtained by breeding.

The CYP2D6 expression cassette was obtained by extraction of a genomic region containing the human *CYP2D6* gene locus from a bacterial artificial chromosome by red/ET recombineering. Sequencing of the genomic fragment showed it to contain different *CYP2D6* polymorphisms, which had previously been found separately in the human population, namely the nucleotide transitions 1023C>T and 2850C>T (leading to the amino acid exchanges T107I and R296C in exon 2 and 6, respectively) and a gene conversion to *CYP2D7* in exon 9 (associated with the amino acid exchanges P469A, T470A, H478S, G479A, F481V, A482S, and S486T) (Supple-

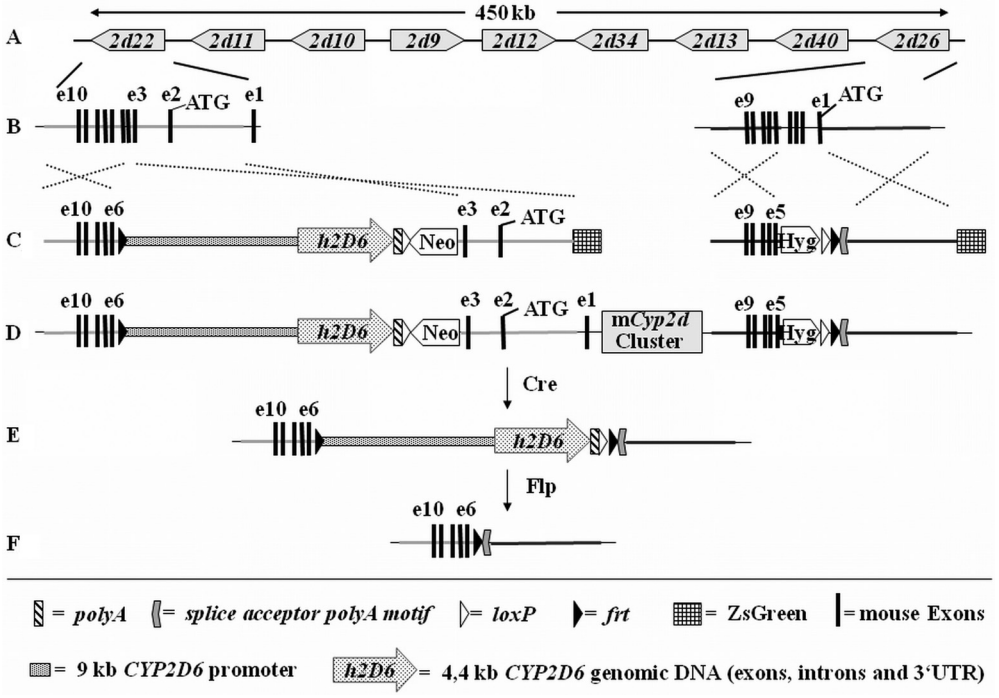

Fig. 1. Strategy for the deletion of the mouse *Cyp2d* cluster and insertion of human CYP2D6 expression cassettes. A, schematic representation of the chromosomal organization and orientation of functional genes within the mouse *Cyp2d* cluster. B, exon/intron structure of *Cyp2d22* and *Cyp2d26*. Exons are represented as black bars and the ATGs mark the translational start sites of both genes. The positions of the targeting arms for homologous recombination are highlighted in light (*Cyp2d22*) and dark gray (*Cyp2d26*), respectively. C, vectors used for targeting of *Cyp2d22* (left) and *Cyp2d26* (right) by homologous recombination. *loxP* and *frt* sites are represented as white and black triangles, respectively. CYP2D6 expression cassettes consisting of a 9-kb promoter sequence (dotted bar) and all exons, introns, and 5′ and 3′ untranslated regions (dotted arrow) are included in the *Cyp2d22* targeting vector. D, genomic organization of the *Cyp2d* cluster in double-targeted ES cells after insertion of the targeting vectors. E, deletion of the mouse *Cyp2d* cluster after Cre-mediated recombination at the *loxP* sites. F, knockout allele of the *Cyp2d* cluster after Flp-mediated deletion of the CYP2D6 expression cassette. For the sake of clarity sequences are not drawn to scale. Hyg, hygromycin expression cassette; Neo, neomycin expression cassette; ZsGreen, ZsGreen expression cassette.

mental Fig. 1) (Johansson et al., 1993, 1994; Masimirembwa et al., 1996). The R296C transition is a frequent polymorphism in all ethnic groups, whereas the T107I and exon 9 gene conversion variants are less common and predominantly found in Africans and African Americans (Masimirembwa et al., 1996; Gaedigk et al., 2006). Of interest, in the *CYP2D6*17*, **40*, and **58* allelic variants, the T107I transition appears in combination with R296C (Masimirembwa et al., 1996; Gaedigk et al., 2002), and in *CYP2D6*63*, R296C and the exon 9 gene conversion are linked (Kramer et al., 2009). However, the combination of all these variants on a single allele has not previously been described and therefore seems to represent a low-frequency polymorphism in the human population. We included this novel genetic variant in one of our targeting vectors and generated CYP2D6-humanized mice according to the strategy described above. We then further changed the coding region of the targeting vector and in this way generated additional humanized mouse lines expressing the CYP2D6.1 and CYP2D6.2 isoforms. The mouse *Cyp2d* cluster was deleted in the different CYP2D6-humanized mouse lines by Cre-mediated recombination, and hereafter they will be referred to as hCYP2D6.N (N for novel), hCYP2D6.1, and hCYP2D6.2. Cyp2d KO mice were obtained from hCYP2D6.N mice by Flp-mediated deletion of the human CYP2D6 expression cassette. Homozygous mice from all transgenic mouse lines appeared normal, could not be distinguished from WT animals, and had normal body weights, liver weights, survival rates, and fertility (data not shown).

Human CYP2D6 and Mouse Cyp2d Expression in Cyp2d KO and CYP2D6-Humanized Mice. To study the expression of the CYP2D6 protein in hCYP2D6.2 mouse tissues, microsomes from WT, Cyp2d KO, and hCYP2D6.2 mice were analyzed by Western blotting using an antibody specific to human CYP2D6. A strong immunoreactive band corresponding to CYP2D6 was detected in liver, duodenum, and jejunum of hCYP2D6.2 mice (Fig. 2A). Ileum microsomes demonstrated a slightly decreased expression compared with that in the other parts of the small intestine. Kidney microsomes showed a low, but detectable, band of CYP2D6. The enzyme level in all other tissues tested was below the limit of quantification by Western blotting. To confirm the absence of CYP2D6 expression in WT and Cyp2d KO mice, Western blotting was performed for liver and small intestine microsomes from these mouse lines as well. No CYP2D6 immunoreactivity could be detected in the liver, duodenum, jejunum, or ileum of WT or Cyp2d KO animals (Fig. 2B).

We also analyzed the combined expression of both mouse Cyp2d and human CYP2D6 isoforms in liver and small intestinal microsomes from WT, Cyp2d KO, and hCYP2D6.2 mice by immunoblot analysis using an antibody recognizing the human and mouse proteins (Fig. 2B). Cyp2d/CYP2D6 proteins were readily detectable in hepatic microsomes of WT and hCYP2D6.2 mice. In the duodenum, the level of Cyp2d/CYP2D6 expression was relatively low in WT animals and much stronger in the hCYP2D6.2 mice. In the jejunum and ileum, Cyp2d/CYP2D6 expression could only be detected in the hCYP2D6.2 but not in WT animals. No Cyp2d/CYP2D6 expression was detected in the liver or small intestine of Cyp2d KO mice. The results for the hCYP2D6.2 line are consistent with the high CYP2D6 expression level in the small intestine of the previously published CYP2D6-humanized mouse model (Miksys et al., 2005).

To further confirm the loss of hepatic mouse *Cyp2d* mRNA expression in the Cyp2d KO and hCYP2D6.2 models, we selected three distant mouse *Cyp2d* genes for TaqMan analysis. mRNA expression of *Cyp2d22*, *Cyp2d26*, and *Cyp2d9*, located either at the outer edges of the cluster or in the

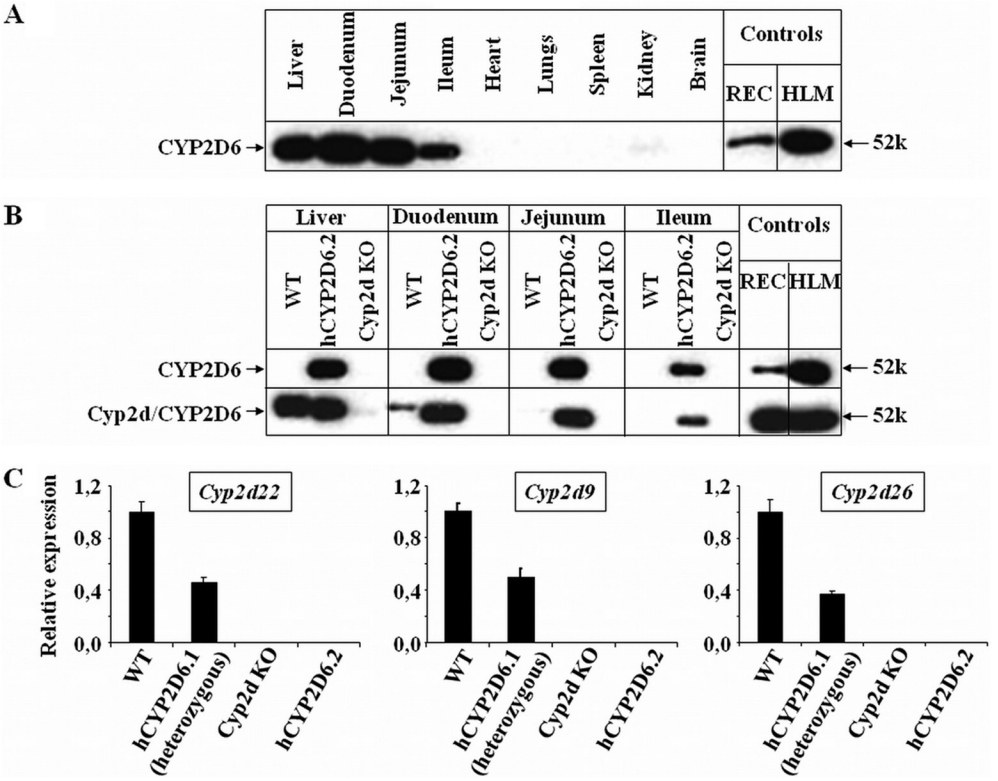

Fig. 2. Analysis of Cyp2d and CYP2D6 expression in WT and different CYP2D transgenic mice. A, human CYP2D6 protein expression in microsomes from different organs of hCYP2D6.2 mice shown by Western blot analysis using a human-specific monoclonal anti-CYP2D6 antibody. The positive controls were HLMs and recombinant CYP2D6 (REC). B, human CYP2D6 (upper lane) and Cyp2d/CYP2D6 (lower lane) protein expression in microsomes from liver, duodenum, jejunum, and ileum of WT, hCYP2D6.2, and Cyp2d KO mice shown by Western blot analysis using a human-specific monoclonal anti-CYP2D6 antibody or an antibody recognizing both human CYP2D6 and mouse Cyp2d proteins, respectively. The positive controls were HLM or recombinant CYP2D6 or Cyp2d22 (REC), respectively. C, expression levels of mouse *Cyp2d22*, *Cyp2d9*, and *Cyp2d26* mRNA in the liver of WT, heterozygous hCYP2D6.1, and homozygous Cyp2d KO and hCYP2D6.2 mice. Relative quantification of mRNA expression with levels in WT mice arbitrarily set as 1. Data are expressed as means ± S.D. (n = 3 mice per genotype).

middle of it, could be readily detected in WT animals but was lost in homozygous Cyp2d KO and hCYP2D6.2 mice (Fig. 2C). We also included heterozygous hCYP2D6.1 mice in this study and, as expected, found an approximate 50% decrease of mRNA levels for all three mouse genes analyzed.

The CYP2D6 and Cyp2d protein expression patterns in the hCYP2D6.N and hCYP2D6.1 mouse lines were indistinguishable from the pattern described in the hCYP2D6.2 animals (data not shown). To compare the level of human *CYP2D6* mRNA among the three humanized mouse lines and also to compare the *CYP2D6* mRNA expression levels in the humanized models with those of *Cyp2d26* in WT animals, TaqMan analysis was performed. This analysis confirmed the pattern of CYP2D6 protein expression described. In the hCYP2D6.1 model, for example, the lowest C_t and ΔC_t values and therefore the highest expression of *CYP2D6* mRNA was observed in liver (mean C_t 18.7), small intestine (21.8), and kidney (22.6) (Supplemental Table 1). With mean C_t values of >27, the *CYP2D6* mRNA expression in all other tissues was very low. A similar pattern of expression was also observed for mouse *Cyp2d26* mRNA in WT animals, with the highest expression in liver (mean C_t 20.1), kidney (21.0), and small intestine (24.1) and negligible expression in all other tissues (mean C_t values >31). The hCYP2D6.2 model showed the same pattern of *CYP2D6* mRNA expression as hCYP2D6.1 mice, and no significant differences in expression levels could be observed in the different tissues analyzed (data not shown). Although the pattern of expression was also the same in the hCYP2D6.N model, *CYP2D6* mRNA levels in liver, small intestine, and kidney of hCYP2D6.N mice was only approximately 50% of that found in hCYP2D6.1 animals (Supplemental Fig. 2).

Catalytic Activities of Microsomes from WT, Cyp2d KO, and CYP2D6-Humanized Mice toward CYP2D6 Substrates. Hepatic microsomes from WT animals had much higher bufuralol 1′-hydroxylase activity than pooled human liver microsomes (HLM). Compared with the WT control, this activity was strongly decreased by ~8.5-fold in Cyp2d KO mice, suggesting that murine Cyp2d proteins catalyze a large majority of this reaction in mouse liver microsomes (Fig. 3A). The catalytic activity of microsomes from the hCYP2D6.2 mice was in between those for WT samples on the one hand and microsomes from Cyp2d KO mice and human liver on the other. The fact that the activity in samples from hCYP2D6.2 mice was ~4.5-fold higher than that in microsomes from Cyp2d KO animals demonstrated that the CYP2D6.2 protein is catalytically active.

The catalytic activities of the different hepatic microsomal preparations for additional CYP2D6 substrates decreased in the following orders: hCYP2D6.2 > WT > HLM > Cyp2d KO for debrisoquine hydroxylation (Fig. 3B); hCYP2D6.2 > WT > Cyp2d KO > HLM for metoprolol α-hydroxylation (Fig. 3C); and WT > hCYP2D6.2 > HLM > Cyp2d KO for dextromethorphan O-demethylation (Fig. 3D). In all cases the activities of samples from WT or hCYP2D6.2 mice were significantly higher and for some compounds markedly increased relative to the microsomes from Cyp2d KO animals. These data demonstrated that mouse Cyp2d proteins have significant activity toward different CYP2D6 substrates, so that WT mice do not generally reflect the human poor metabolizer phenotype as suggested previously. The data also provide further evidence for the catalytic activity of the expressed CYP2D6 protein in the hCYP2D6.2 mouse line. Furthermore, the results show that there is a significant species difference between mice and humans in the catalytic activity toward different CYP2D6 substrates. Whereas bufuralol and dextromethorphan are preferred substrates for the mouse enzymes, debrisoquine and metoprolol are more readily metabolized by human CYP2D6.

To assess potential differences in the response to the CYP2D6 inhibitor quinidine between mouse and human CYP2D proteins, we investigated the effect of this compound on microsomal activity toward different CYP2D substrates. Quinidine markedly inhibited bufuralol 1′-hydroxylation, debrisoquine 4′-hydroxylation, metoprolol α-hydroxylation, and dextromethorphan O-demethylation activity of both HLM

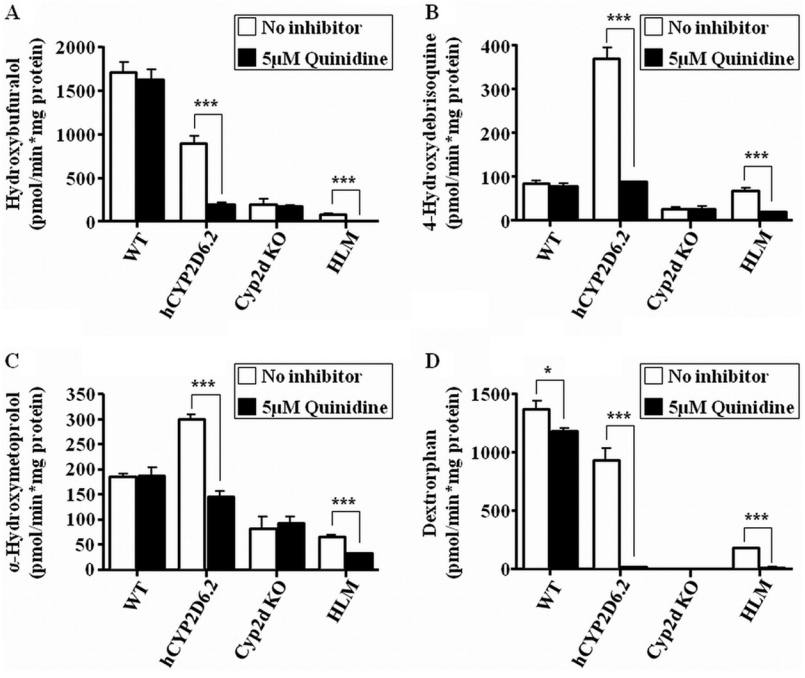

Fig. 3. In vitro metabolism of CYP2D6 probe substrates by liver microsomes from WT, hCYP2D6.2, and Cyp2d KO mice and humans. Bufuralol 1′-hydroxylation (A), debrisoquine 4-hydroxylation (B), metoprolol α-hydroxylation (C), and dextromethorphan O-demethylation (D) either without inhibitor (□) or during coincubation with 5 μM quinidine (■) are shown. Data are expressed as means ± S.D. ($n = 3$ for all mouse lines). Activities of quinidine-treated samples were compared with those from the corresponding control group using a Student's t test (two-sided). *, $p < 0.05$; ***, $p < 0.001$, statistically different from control.

and of microsomes from the hCYP2D6.2 mice (Fig. 3, A–D). In microsomes from WT animals, dextromethorphan O-demethylation was very slightly inhibited (1.2-fold), with no effect on the metabolism of the other substrates. In agreement with literature reports (Martignoni et al., 2006), the data therefore suggest a high selectivity of this inhibitor for human versus murine CYP2D proteins.

Metabolism studies were also conducted using microsomes from the jejunum of WT, hCYP2D6.2, and Cyp2d KO mice. No major differences in the results obtained from liver microsomes were observed in these studies (Supplemental Fig. 3).

To assess the catalytic activity of the novel CYP2D6 variant, we then analyzed the hydroxylation of different CYP2D6 substrates by liver microsomes from the hCYP2D6.N mice. The debrisoquine hydroxylase activity of microsomes from hCYP2D6.N mice was higher (1.8-fold) than that of microsomes from the Cyp2d KO line ($p < 0.05$), indicating that the polymorphic variant of CYP2D6 had some activity toward this substrate (Fig. 4A). However, in contrast to the samples from hCYP2D6.2 mice, the activity was much lower than that from WT microsomes or HLM, indicating that the catalytic function of the novel CYP2D6 variant is impaired. This observation was further substantiated in that dextromethorphan O-demethylation in microsomes from hCYP2D6.N mice, which was 10 times higher than that in Cyp2d KO microsomes, was markedly lower than that in HLM (Fig. 4B). Of interest, there was no difference in the rate of bufuralol 1′-hydroxylation or metoprolol α-hydroxylation between the microsomes from Cyp2d KO and hCYP2D6.N mice (data not shown), suggesting that the novel CYP2D6 variant is catalytically inactive toward those substrates. The comparison of relative catalytic activities of mouse Cyp2d, human CYP2D6.2, and human CYP2D6.N in mouse liver microsomes toward the different substrates tested is summarized in Supplemental Table 2.

Catalytic activity of microsomes from hCYP2D6.1 mice was only tested in heterozygous mice, which still contain one WT allele of the mouse *Cyp2d* cluster. Compared with WT samples, debrisoquine 4′-hydroxylase activity in microsomes from heterozygous hCYP2D6.1 mice was slightly increased, and this activity was significantly inhibited by quinidine (Supplemental Fig. 4A). These data indicate that the CYP2D6 protein expressed in this model is functionally active and susceptible to the inhibitor. For bufuralol 1′-hydroxylase activity, the inhibitory effect of quinidine on microsomes from heterozygous hCYP2D6.1 mice was marginal and not statistically significant (Supplemental Fig. 4B). The likely reason for this observation is the dominant effect of the remaining mouse Cyp2d proteins toward this substrate.

Pharmacokinetics of CYP2D Substrates and In Vivo Effects of Quinidine in WT and hCYP2D6.2 Mice. We compared the pharmacokinetics of bufuralol in WT and hCYP2D6.2 mice and analyzed the pharmacokinetic changes after coadministration of quinidine (Fig. 5A). Consistent with the higher bufuralol 1′-hydroxylase activity of microsomes from WT mice compared with those from hCYP2D6.2 animals, bufuralol exposure was increased in transgenic mice, suggesting faster elimination of the compound in WT animals. Cotreatment with quinidine increased the bufuralol exposure in hCYP2D6.2 mice but not in WT animals. In agreement with the in vitro results, quinidine therefore is also a selective inhibitor of human CYP2D6 in vivo.

In contrast to the results for bufuralol, the exposure to debrisoquine was much higher in WT mice than in hCYP2D6.2 animals (Fig. 5B). This finding is consistent with the higher debrisoquine 4′-hydroxylase activity in microsomes from the humanized mice. In fact, the debrisoquine area under the concentration time curve (AUC) was markedly (>10 times) decreased in hCYP2D6.2 mice compared with WT animals (Fig. 5C). There was no statistically significant difference between the AUC of debrisoquine in WT and Cyp2d KO mice.

To assess the differences in the exposure to a CYP2D metabolite among the different mouse lines, the pharmacokinetics of the 4-hydroxydebrisoquine metabolite in debrisoquine-treated WT, hCYP2D6.2, and Cyp2d KO mice was determined (Fig. 5D). The metabolite exposure in these mouse lines was a mirror image of the exposure to the parent compound. The AUC of 4-hydroxydebrisoquine in hCYP2D6.2 mice was markedly (>10 times) higher than that in WT or Cyp2d KO animals (Fig. 5E). We also determined the relative concentrations of 4-hydroxydebrisoquine expressed as a percentage of the parent compound in urine samples. The relative concentration of the metabolite was markedly (~146 times) higher in hCYP2D6.2 mice compared with that in WT animals, whereas in Cyp2d KO mice, the relative concentration was slightly (~3 times) lower than that in WT animals.

Comparison of Debrisoquine and 4-Hydroxydebrisoquine Ratios in WT, Cyp2d KO, and hCYP2D6.2 Mice with Different Human CYP2D6 Metabolizer Phenotypes. In humans, CYP2D6 phenotypes have been classified on the basis of the ratio of debrisoquine to 4-hydroxydebrisoquine in urine, the so-called urine metabolic ratio (MR). The MR is inversely correlated with the number of active CYP2D6 copies (Dalén et al., 1999). The observed MR in individuals with different CYP2D6 metabolizer phenotypes is re-

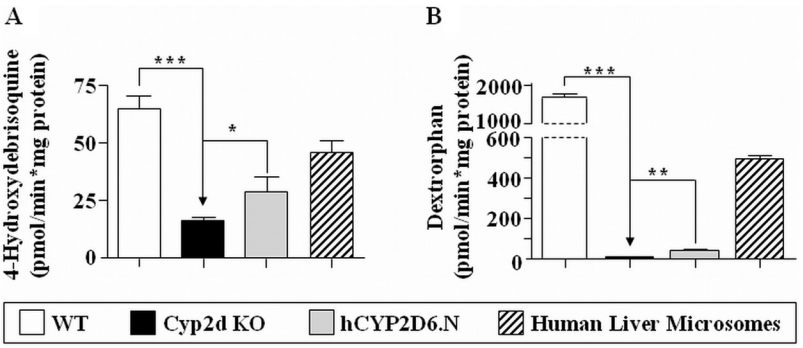

Fig. 4. In vitro metabolism of CYP2D6 substrates by liver microsomes from WT, Cyp2d KO, and hCYP2D6.N mice. A, debrisoquine 4-hydroxylation. B, dextromethorphan O-demethylation. Data shown are means ± S.D. ($n = 3$). Activities of samples from Cyp2d KO mice were compared with those from WT and hCYP2D6.N animals using a Student's t test (two-sided). *, $p < 0.05$; **, $p < 0.01$; ***, $p < 0.001$, statistically different from control.

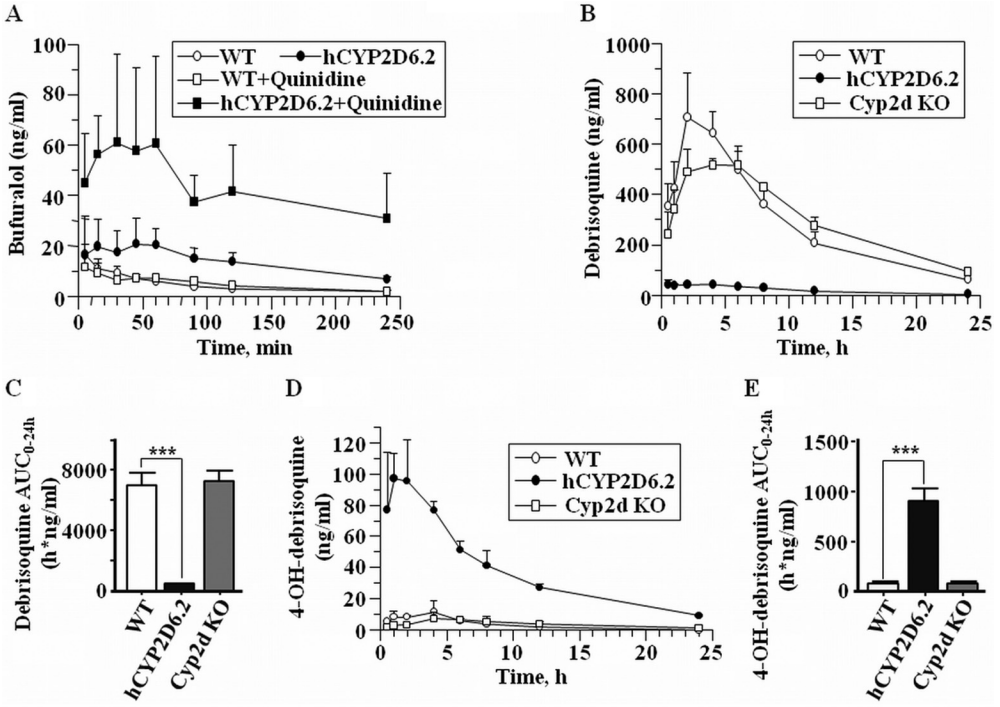

Fig. 5. Pharmacokinetics of CYP2D substrates and metabolites in WT, hCYP2D6.2, and Cyp2d KO mice. Bufuralol (with and without coadministration of quinidine) (A) and debrisoquine concentration (B) versus time dependence. C, AUC (between 0 and 24 h) for debrisoquine. D, 4-hydroxydebrisoquine concentration versus time dependence. E, AUC (between 0 and 24 h) for 4-hydroxydebrisoquine. Data shown are means ± S.D. in all cases (with n = 3 mice/genotype and treatment group). AUCs of debrisoquine (C) and hydroxydebrisoquine (E) in hCYP2D6.2 mice were compared with those in WT animals using a Student's t test (two-sided). ***, statistically different from control at $p < 0.001$.

ported to be 23 to 131 for poor metabolizers with no functional CYP2D6, 0.4 to 12.6 for intermediate metabolizers with 1 active copy of CYP2D6, 0.13 to 1.01 for extensive metabolizers with 2 active copies of CYP2D6, 0.03 to 0.18 for ultrarapid metabolizers with 3 or 4 active CYP2D6 copies, and 0.01 in a subject with 13 active enzyme copies (Dahl et al., 1992; Dalén et al., 1999, 2003). When urine debrisoquine/4-hydroxydebrisoquine ratios in mouse urine are compared with the human data (Fig. 6A), both WT (MR of 13.9–18.8) and Cyp2d KO (MR of 30–71) mice resemble human poor metabolizers, whereas hCYP2D6.2 animals with a MR of 0.1 to 0.14 fall into the overlapping area of both extensive and ultrarapid metabolizers.

In correlation to the urine ratios, a significant difference in plasma AUC ratios of debrisoquine to 4-hydroxydebrisoquine was also observed across the spectrum of human CYP2D6 polymorphisms (Dalén et al., 1999). In poor metabolizers the plasma 4-hydroxydebrisoqine concentration was below the limit of quantification. Because this limit was used instead of a real value for the calculation, the resultant mean ratio of 42 was considered as an underestimation. In this regard, both in WT mice with a mean AUC ratio of 90 and in Cyp2d KO animals with a mean AUC ratio of 93, these values were similar to those observed in plasma of human poor metabolizers (Fig. 6B). Consistent with the urine metabolic ratios described above, the mean AUC ratio of 0.56 in the hCYP2D6.2 mice was between the established ratios of 0.77 in extensive human metabolizers and 0.46 in ultrarapid metabolizers.

Classification of WT, Cyp2d KO, and hCYP2D6.2 Mice into the Human CYP2D6 Metabolizer Spectrum for Bufuralol. Although WT mice metabolize some CYP2D6 substrates very poorly, this is not the case for all substrates. As discussed above, WT mice are therefore not equivalent to human poor metabolizers. To establish whether the Cyp2d KO mice are a more reliable model for this human phenotype, we compared the AUC ratios for bufuralol in Cyp2d KO versus WT and Cyp2d KO versus hCYP2D6.2 animals with human poor/extensive metabolizer AUCs calculated from published data (Dayer et al., 1985). Human bufuralol AUC ratios were determined for three individual poor metabolizers versus an "average" extensive metabolizer, as a mean of seven individual extensive metabolizers. The AUC ratio of 17.5 for the human poor metabolizer with the lowest bufuralol clearance was similar to the ratio of 13.6 observed for Cyp2d KO/WT mice, and the ratios for two other poor metabolizers (2.8 and 5.8) were in the range of the 4.3 ratio determined for Cyp2d KO/hCYP2D6.2 animals (Supplemental Fig. 5). Therefore, for bufuralol-like substrates, Cyp2d KO rather than WT mice seem to represent the human poor metabolizer phenotype, whereas both WT and hCYP2D6.2 animals can be considered to reflect the extensive metabolizers of the human spectrum.

Discussion

Human CYP2D6 plays a major role in the metabolism and disposition of up to 25% of currently used drugs. Although a number of in vitro approaches have been developed to predict CYP2D6 involvement in drug disposition (Johnson et al.,

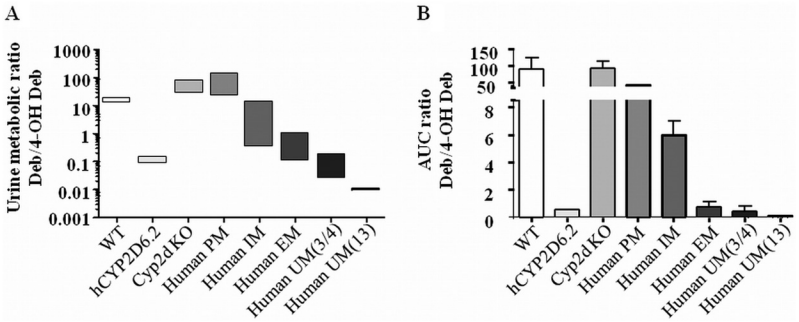

Fig. 6. Comparison of debrisoquine (Deb) to 4-hydroxydebrisoquine (4-OH Deb) ratios in different mouse lines and various human CYP2D6 metabolizers. Urine metabolic ratios (A) and AUC (0–24 h whole blood for mice and 0–8 h plasma for humans) ratios (B) in WT, hCYP2D6.2, and Cyp2d KO mice and in human CYP2D6 poor (PM), intermediate (IM), efficient (EM), and ultrarapid (UM) metabolizers. UM(3/4) and UM(13) carry 3 or 4 and 13 active copies of CYP2D6, respectively.

2006; Pritchard et al., 2006), it is clear that there are many ways that variation in the expression can affect efficiency and side effects, which cannot be predicted from in vitro studies (Almond et al., 2009). CYP2D6 function in humans is variable because of individual differences in the level of CYP2D6 expression (Forrester et al., 1992), genetic polymorphism, and drug-drug interactions. Many allelic variants of this enzyme have been identified as affecting catalytic function to a greater or lesser extent. At one end of the spectrum, there are alleles devoid of CYP2D6 activity, which have been associated with the CYP2D6 poor metabolizer phenotype. The clinical importance of this phenotype can be illustrated by its effect on the efficacy of tamoxifen for the prevention and treatment of steroid hormone receptor-positive breast cancer. Because tamoxifen requires an enzymatic activation for the formation of its pharmacologically active metabolites, primarily by CYP2D6, poor metabolizer phenotypes are associated with higher recurrence rates, and it was suggested that CYP2D6 genotyping before treatment may open new avenues for individualizing endocrine treatment (Brauch et al., 2009; Hoskins et al., 2009). Although extensive metabolizers with two active copies of CYP2D6 are most prevalent in the human population, certain allelic CYP2D6 variants do contain three or more active copies of human CYP2D6, giving rise to ultrarapid metabolizers (Sachse et al., 1997). It is well known that the disposition and action of a wide range of different compounds depend on the individual CYP2D6 phenotype (Kroemer and Eichelbaum, 1995).

To better define potential differences in the in vivo response to drugs and chemicals as a result of the variability in CYP2D6 expression or catalytic activity, we generated transgenic mice devoid of *Cyp2d* genes or humanized with different allelic variants of human *CYP2D6*. Like the *Cyp3a*(−/−) mice described previously (van Herwaarden et al., 2007), *Cyp2d* cluster knockout mice were viable and fertile and did not display any physiological abnormalities. The CYP2D6-humanized mouse lines were generated by a novel approach that allows mice containing allelic variants of CYP2D6 to be expressed while at the same time deleting the nine mouse *Cyp2d* genes. In the present study, we used this approach to express different CYP2D6 protein isoforms under control of the human *CYP2D6* promoter, resulting in hCYP2D6.1, hCYP2D6.2, and hCYP2D6.N mice. This approach gave expression in tissues in which CYP2D6 has been detected in humans, i.e., in liver, gut, and kidney (Madani et al., 1999; Miksys et al., 2005). The expression of CYP2D6 in humans varies up to 16-fold among individuals (Forrester et al., 1992) and is poorly understood to date (Cairns et al., 1996). Although in contrast with many other cytochrome P450 proteins involved in drug metabolism, CYP2D6 expression seems to be noninducible by xenobiotic compounds, but age and genetic factors constitute significant determinants of interindividual differences in CYP2D6 expression (Stevens et al., 2008). The humanized mouse models described in the present work might help to further elucidate how this gene is regulated. However, it should be noted that the expression level of CYP2D6 in liver and small intestine of the CYP2D6-humanized mouse lines was similar, whereas in humans the hepatic CYP2D6 content has been proposed to be more pronounced (Paine et al., 2006). Further studies comparing mouse and human samples will be required to analyze potential regional differences in the CYP2D6 expression level between the transgenic mice and humans. It is interesting to note that, although the expression level of the human mRNA in the hCYP2D6.1 and hCYP2D6.2 mice was comparable, it was decreased by approximately 50% in the hCYP2D6.N model. Whether this effect is due to changes in mRNA transcription or stability is currently unknown but may indicate that polymorphic allelic variants contribute to the CYP2D6 metabolizer phenotype by affecting the expression level of the mRNA, in addition to determining differences in the catalytic activity of the protein.

From previous studies, it has not been clear how CYP2D6-related metabolism is represented in mice. The initially observed selective deficiency of debrisoquine 4-hydroxylase activity in mice (Masubuchi et al., 1997; Corchero et al., 2001) was used as a basis to consider WT mice as being representative of the poor metabolizer phenotype (Yu et al., 2004). This is not the case, however, for all substrates, because mouse liver microsomes demonstrated oxidative activities against several CYP2D substrates comparable with those in rat and human liver microsomes (Masubuchi et al., 1997; Bogaards et al., 2000). In the present study, the profound decrease in the rate of oxidation of bufuralol, dextromethorphan, and metoprolol in liver microsomes from the Cyp2d KO mice demonstrates that, similar to humans, isoforms from the Cyp2d subfamily are the major enzymes involved in the metabolism of these CYP2D substrates. Indeed, all the CYP2D6 substrates tested were metabolized at higher rates in mouse than in human liver microsomes. In agreement with previous work, bufuralol hydroxylation in mouse liver microsomes was one of the highest relative to that of other species (Bogaards et al., 2000), being 10 times higher than in pooled human liver microsomes. Our studies illustrate the significant species differences in the metabolism of different CYP2D6 substrates between mouse Cyp2d enzymes and human CYP2D6, demonstrating the difficulty in extrapolating such results from mice to humans.

To further assess which human metabolizer phenotypes might be represented by the different mouse lines used in this study, a comparison between published clinical pharmacokinetic data and the mouse models was undertaken for the two CYP2D6 probe substrates debrisoquine and bufuralol. This analysis showed that the MR of debrisoquine to its 4-hydroxydebrisoquine metabolite in urine of human poor metabolizers was similar to the corresponding MR in Cyp2d KO mice. In contrast, the MR of hCYP2D6.2 animals overlapped with both extensive and ultrarapid human metabolizers. Comparable results were obtained when plasma AUC ratios of debrisoquine to 4-hydroxydebrisoquine were calculated. For bufuralol, the AUC ratio for Cyp2d KO/hCYP2D6.2 mice was in a range similar to those calculated for different human poor/extensive metabolizer AUCs. Therefore, for both debrisoquine and bufuralol, the Cyp2d KO and hCYP2D6.2 models represented the poor and extensive to ultrarapid human metabolizer phenotypes, respectively.

We have also demonstrated that the human CYP2D6 inhibitor quinidine decreases CYP2D6-mediated metabolism in vivo and in microsomal fractions derived from hCYP2D6.2 mice. In contrast, no inhibitory effect was observed in WT animals. Therefore, the hCYP2D6.2 model might more reliably predict drug-drug interactions in humans.

The *CYP2D6* allele incorporated in the hCYP2D6.N model has not been described in the literature before. In all likeli-

hood, it represents a very rare *CYP2D6* variant. It encodes a protein that combines a number of known amino acid changes that have not previously been found on the same allele, but that are partially linked in certain allelic variants (e.g., *CYP2D6*17*, **40*,**58*, and **6*) (Masimirembwa et al., 1996; Gaedigk et al., 2002). Compared with liver microsomes from Cyp2d KO animals, samples from hCYP2D6.N mice had slightly but statistically significant increased catalytic activities toward debrisoquine and dextromethorphan, whereas no difference in bufuralol 1′-hydroxylation or metoprolol α-hydroxylation activities could be measured. The R296C amino acid change in this variant is common in the human population but does not seem to significantly alter CYP2D6 activity (Johansson et al., 1993). However, the T107I polymorphism alone or in combination with R296C can significantly decrease catalytic activity (Oscarson et al., 1997). In addition, it has been speculated that the amino acid exchanges associated with the *CYP2D7* exon 9 conversion in the *CYP2D6*36* allelic variant also found in CYP2D6.N will not significantly affect the activity (Johansson et al., 1994), but the enzymatic consequences of this polymorphism are not well established. The data generated in the present study suggest that the combination of amino acid changes causes a marked reduction in CYP2D6 catalytic activity.

In conclusion, a new method was described to create humanized mouse lines deleted for multigene families of linked mouse genes. In the present example, this approach was used to generate mouse lines expressing different polymorphic variants of CYP2D6 as well as a mouse line with a deletion of the mouse *Cyp2d* gene cluster. The different mouse lines reflect a number of different human CYP2D6 variants, which will be useful tools in modeling the range of potential drug responses in different CYP2D6 metabolizer phenotypes in humans.

Acknowledgments

We thank Sandra Buechel, Sylvia Krueger, and Anja Mueller (TaconicArtemis, Cologne, Germany) and Barbara Elcombe, Marie Bowers, Antony Purvis, Corinne Haines, Enateri Alakpa, and Sol Gibson (CXR Biosciences, Dundee, UK) for technical assistance.

Authorship Contributions

Participated in research design: Scheer, Kapelyukh, and Wolf.
Conducted experiments: Kapelyukh, McEwan, Beuger, and Rode.
Performed data analysis: Scheer, Kapelyukh, Beuger, and Wolf.
Wrote or contributed to the writing of the manuscript: Scheer, Kapelyukh, Stanley, and Wolf.

References

Almond LM, Yang J, Jamei M, Tucker GT, and Rostami-Hodjegan A (2009) Towards a quantitative framework for the prediction of DDIs arising from cytochrome P450 induction. *Curr Drug Metab* **10:**420–432.
Bogaards JJ, Bertrand M, Jackson P, Oudshoorn MJ, Weaver RJ, van Bladeren PJ, and Walther B (2000) Determining the best animal model for human cytochrome P450 activities: a comparison of mouse, rat, rabbit, dog, micropig, monkey and man. *Xenobiotica* **30:**1131–1152.
Bradford LD (2002) CYP2D6 allele frequency in European Caucasians, Asians, Africans and their descendants. *Pharmacogenomics* **3:**229–243.
Brauch H, Mürdter TE, Eichelbaum M, and Schwab M (2009) Pharmacogenomics of tamoxifen therapy. *Clin Chem* **55:**1770–1782, 2009.
Brockmöller J and Tzvetkov MV (2008) Pharmacogenetics: data, concepts and tools to improve drug discovery and drug treatment. *Eur J Clin Pharmacol* **64:**133–157.
Cairns W, Smith CA, McLaren AW, and Wolf CR (1996) Characterization of the human cytochrome P4502D6 promoter. A potential role for antagonistic interactions between members of the nuclear receptor family. *J Biol Chem* **271:**25269–25276.
Cheung C and Gonzalez FJ (2008) Humanized mouse lines and their application for prediction of human drug metabolism and toxicological risk assessment. *J Pharmacol Exp Ther* **327:**288–299.
Corchero J, Granvil CP, Akiyama TE, Hayhurst GP, Pimprale S, Feigenbaum L, Idle JR, and Gonzalez FJ (2001) The CYP2D6 humanized mouse: effect of the human CYP2D6 transgene and HNF4α on the disposition of debrisoquine in the mouse. *Mol Pharmacol* **60:**1260–1267.
Dahl ML, Johansson I, Palmertz MP, Ingelman-Sundberg M, and Sjöqvist F (1992) Analysis of the CYP2D6 gene in relation to debrisoquin and desipramine hydroxylation in a Swedish population. *Clin Pharmacol Ther* **51:**12–17.
Dalén P, Dahl ML, Eichelbaum M, Bertilsson L, and Wilkinson GR (1999) Disposition of debrisoquine in Caucasians with different CYP2D6-genotypes including those with multiple genes. *Pharmacogenetics* **9:**697–706.
Dalén P, Dahl ML, Roh HK, Tybring G, Eichelbaum M, Wilkinson GR, and Bertilsson L (2003) Disposition of debrisoquine and nortriptyline in Korean subjects in relation to CYP2D6 genotypes, and comparison with Caucasians. *Br J Clin Pharmacol* **55:**630–634.
Dayer P, Balant L, Kupfer A, Striberni R, and Leemann T (1985) Effect of oxidative polymorphism (debrisoquine/sparteine type) on hepatic first-pass metabolism of bufuralol. *Eur J Clin Pharmacol* **28:**317–320.
de Leon J, Armstrong SC, and Cozza KL (2006) Clinical guidelines for psychiatrists for the use of pharmacogenetic testing for CYP450 2D6 and CYP450 2C19. *Psychosomatics* **47:**75–85.
Eichelbaum M, Ingelman-Sundberg M, and Evans WE (2006) Pharmacogenomics and individualized drug therapy. *Annu Rev Med* **57:**119–137.
Forrester LM, Henderson CJ, Glancey MJ, Back DJ, Park BK, Ball SE, Kitteringham NR, McLaren AW, Miles JS, and Skett P, et al. (1992) Relative expression of cytochrome P450 isoenzymes in human liver and association with the metabolism of drugs and xenobiotics. *Biochem J* **281:**359–368.
Gaedigk A, Bradford LD, Alander SW, and Leeder JS (2006) CYP2D6*36 gene arrangements within the cyp2d6 locus: association of CYP2D6*36 with poor metabolizer status. *Drug Metab Dispos* **34:**563–569.
Gaedigk A, Bradford LD, Marcucci KA, and Leeder JS (2002) Unique CYP2D6 activity distribution and genotype-phenotype discordance in black Americans. *Clin Pharmacol Ther* **72:**76–89.
Gonzalez FJ, Skoda RC, Kimura S, Umeno M, Zanger UM, Nebert DW, Gelboin HV, Hardwick JP, and Meyer UA (1988) Characterization of the common genetic defect in humans deficient in debrisoquine metabolism. *Nature* **331:**442–446.
Gough AC, Miles JS, Spurr NK, Moss JE, Gaedigk A, Eichelbaum M, and Wolf CR (1990) Identification of the primary gene defect at the cytochrome P450 CYP2D locus. *Nature* **347:**773–776.
Hogan BL, Beddington RS, Costantini F, and Lacy E (1994) *Manipulating the Mouse Embryo: A Laboratory Manual*, pp 253–289, Cold Spring Harbor Laboratory, Plainview, NY.
Hoskins JM, Carey LA, and McLeod HL (2009) CYP2D6 and tamoxifen: DNA matters in breast cancer. *Nat Rev Cancer* **9:**576–586.
Johansson I, Lundqvist E, Bertilsson L, Dahl ML, Sjöqvist F, and Ingelman-Sundberg M (1993) Inherited amplification of an active gene in the cytochrome P450 CYP2D locus as a cause of ultrarapid metabolism of debrisoquine. *Proc Natl Acad Sci USA* 90:11825–11829.
Johansson I, Oscarson M, Yue QY, Bertilsson L, Sjöqvist F, and Ingelman-Sundberg M (1994) Genetic analysis of the Chinese cytochrome P4502D locus: characterization of variant CYP2D6 genes present in subjects with diminished capacity for debrisoquine hydroxylation. *Mol Pharmacol* **46:**452–459.
Johnson TN, Rostami-Hodjegan A, and Tucker GT (2006) Prediction of the clearance of eleven drugs and associated variability in neonates, infants and children. *Clin Pharmacokinet* **45:**931–956.
Kramer WE, Walker DL, O'Kane DJ, Mrazek DA, Fisher PK, Dukek BA, Bruflat JK, and Black JL (2009) CYP2D6: novel genomic structures and alleles. *Pharmacogenet Genomics* **19:**813–822.
Kroemer HK and Eichelbaum M (1995) "It's the genes, stupid". Molecular bases and clinical consequences of genetic cytochrome P450 2D6 polymorphism. *Life Sci* **56:**2285–2298.
Lin JH (2008) Applications and limitations of genetically modified mouse models in drug discovery and development. *Curr Drug Metab* **9:**419–438.
Madani S, Paine MF, Lewis L, Thummel KE, and Shen DD (1999) Comparison of CYP2D6 content and metoprolol oxidation between microsomes isolated from human livers and small intestines. *Pharm Res* **16:**1199–1205.
Martignoni M, Groothuis GM, and de Kanter R (2006) Species differences between mouse, rat, dog, monkey and human CYP-mediated drug metabolism, inhibition and induction. *Expert Opin Drug Metab Toxicol* **2:**875–894.
Masimirembwa C, Persson I, Bertilsson L, Hasler J, and Ingelman-Sundberg M (1996) A novel mutant variant of the CYP2D6 gene (*CYP2D6*17*) common in a black African population: association with diminished debrisoquine hydroxylase activity. *Br J Clin Pharmacol* **42:**713–719.
Masubuchi Y, Iwasa T, Hosokawa S, Suzuki T, Horie T, Imaoka S, Funae Y, and Narimatsu S (1997) Selective deficiency of debrisoquine 4-hydroxylase activity in mouse liver microsomes. *J Pharmacol Exp Ther* **282:**1435–1441.
McLaughlin LA, Dickmann LJ, Wolf CR, and Henderson CJ (2008) Functional expression and comparative characterization of nine murine cytochromes P450 by fluorescent inhibition screening. *Drug Metab Dispos* **36:**1322–1331.
Miksys SL, Cheung C, Gonzalez FJ, and Tyndale RF (2005) Human CYP2D6 and mouse CYP2Ds: organ distribution in a humanized mouse model. *Drug Metab Dispos* **33:**1495–1502.
Nelson DR, Zeldin DC, Hoffman SM, Maltais LJ, Wain HM, and Nebert DW (2004) Comparison of cytochrome P450 (CYP) genes from the mouse and human genomes, including nomenclature recommendations for genes, pseudogenes and alternative-splice variants. *Pharmacogenetics* **14:**1–18.
Oscarson M, Hidestrand M, Johansson I, and Ingelman-Sundberg M (1997) A combination of mutations in the *CYP2D6*17* (*CYP2D6Z*) allele causes alterations in enzyme function. *Mol Pharmacol* **52:**1034–1040.
Paine MF, Hart HL, Ludington SS, Haining RL, Rettie AE, and Zeldin DC (2006) The human intestinal cytochrome P450 "pie". *Drug Metab Dispos* **34:**880–886.

Pritchard MP, McLaughlin L, and Friedberg T (2006) Establishment of functional human cytochrome P450 monooxygenase systems in *Escherichia coli*. *Methods Mol Biol* **320:**19–29.
Sachse C, Brockmöller J, Bauer S, and Roots I (1997) Cytochrome P450 2D6 variants in a Caucasian population: allele frequencies and phenotypic consequences. *Am J Hum Genet* **60:**284–295.
Sakuyama K, Sasaki T, Ujiie S, Obata K, Mizugaki M, Ishikawa M, and Hiratsuka M (2008) Functional characterization of 17 CYP2D6 allelic variants (CYP2D6.2, 10, 14A-B, 18, 27, 36, 39, 47–51, 53–55, and 57). *Drug Metab Dispos* **36:**2460–2467.
Scheer N, Ross J, Rode A, Zevnik B, Niehaves S, Faust N, and Wolf CR (2008) A novel panel of mouse models to evaluate the role of human pregnane X receptor and constitutive androstane receptor in drug response. *J Clin Invest* **118:**3228–3239.
Smith G, Modi S, Pillai I, Lian LY, Sutcliffe MJ, Pritchard MP, Friedberg T, Roberts GC, and Wolf CR (1998) Determinants of the substrate specificity of human cytochrome P-450 CYP2D6: design and construction of a mutant with testosterone hydroxylase activity. *Biochem J* **331:**783–792.
Stevens JC, Marsh SA, Zaya MJ, Regina KJ, Divakaran K, Le M, and Hines RN (2008) Developmental changes in human liver CYP2D6 expression. *Drug Metab Dispos* **36:**1587–1593.
Thuerauf N and Lunkenheimer J (2006) The impact of the CYP2D6-polymorphism on dose recommendations for current antidepressants. *Eur Arch Psychiatry Clin Neurosci* **256:**287–293.
van Herwaarden AE, Wagenaar E, van der Kruijssen CM, van Waterschoot RA, Smit JW, Song JY, van der Valk MA, van Tellingen O, van der Hoorn JW, Rosing H, et al. (2007) Knockout of cytochrome P450 3A yields new mouse models for understanding xenobiotic metabolism. *J Clin Invest* **117:**3583–3592.
Yu AM, Idle JR, and Gonzalez FJ (2004) Polymorphic cytochrome P450 2D6: humanized mouse model and endogenous substrates. *Drug Metab Rev* **36:**243–277.
Zanger UM, Raimundo S, and Eichelbaum M (2004) Cytochrome P450 2D6: overview and update on pharmacology, genetics, biochemistry. *Naunyn Schmiedebergs Arch Pharmacol* **369:**23–37.
Zhang Y, Buchholz F, Muyrers JP, and Stewart AF (1998) A new logic for DNA engineering using recombination in *Escherichia coli*. *Nat Genet* **20:**123–128.

Address correspondence to: Dr. Nico Scheer, TaconicArtemis, Neurather Ring 1, 51063 Köln, Germany. E-mail: nico.scheer@taconicartemis.com